IEEE Access
Multidisciplinary ⋮ Rapid Review ⋮ Open Access Journal

Received 12 November 2023, accepted 27 November 2023, date of publication 30 November 2023,
date of current version 6 December 2023.

Digital Object Identifier 10.1109/ACCESS.2023.3337998

RESEARCH ARTICLE

Sub-Seasonal Precipitation Bias-Correction in Thailand Using Attention U-Net With Seasonal and Meteorological Effects

TANATORN FAIJAROENMONGKOL[1], KANOKSRI SARINNAPAKORN[2], AND PEERAPON VATEEKUL[1], (Member, IEEE)
[1]Department of Computer Engineering, Faculty of Engineering, Chulalongkorn University, Pathum Wan, Bangkok 10330, Thailand
[2]Hydro-Informatics Institute, Bangkok 10900, Thailand

Corresponding author: Peerapon Vateekul (peerapon.v@chula.ac.th)

ABSTRACT There have been many attempts to forecast sub-seasonal to seasonal (S2S) precipitation. One of them is the Climate Forecast System version 2 (CFSv2) model; however, a bias correction must be applied before CFSv2 data can be used in each local region. In this research, we aim to address the S2S precipitation forecasting using our new bias correction on CFSv2 data. Our model is based on the deep learning model: Attention U-Net having two proposed enhancements: (*i*) a multi-scale residual block to learn patterns on different scales and (*ii*) a combination of customized regression loss and classification loss. Further, we apply a log scaler to reduce the impact of skewness in the data. Finally, seasonal and meteorological effects are provided as additional input for our model. CFSv2 is employed as a dataset to be corrected in our study, while rainfall data from Thailand's Hydro-Informatics Institute (HII) is served as the ground truth. In the result, it demonstrates that our model outperforms two baseline models: namely, a linear-downscaling technique (traditional approach) and a traditional Attention U-Net model. Our model's root mean square error (RMSE) and temporal correlation coefficient (TCC) improve about 8.65% and 13.77% respectively, over the linear-downscaling technique. Besides the results of the Attention U-Net model reveal that our model's RMSE and TCC improve by about 15.56% and 12.06%, respectively.

INDEX TERMS Sub-seasonal precipitation forecasting, bias-correction.

I. INTRODUCTION

Precipitation is an important factor in water management and agriculture in Thailand. A reliable precipitation forecast is critical in a climate forecasting system. Precipitation forecasting, in particular, is carried out over a long period of time. Some periods are influenced by short-term atmospheric phenomena (weather forecasts), while others are influenced by long-term atmospheric phenomena (climate forecasts). As evidenced by previous studies [1], these differences create a noticeable gap in weather-climate forecasting at the sub-seasonal to seasonal (S2S) scale. Improving the accuracy of S2S precipitation prediction has become critical to closing this gap and improving the performance of various applications such as agriculture, water resource management, and disaster management. Nonetheless, S2S precipitation forecasting poses research challenges owing to the presence of intra-seasonal phenomena such as monsoon systems.

Over the past decades, many image-like datasets for rainfall prediction have been created using a wide range of methodologies, such as dynamic forecasting models, analog methods, and machine learning models. Among the techniques to forecast precipitation, a dynamic forecasting model is one of the most reliable and globally accepted methods. The ability of dynamic forecasting models like Climate Forecast System version 2 (CFSv2) [2] and European Centre for Mid-Range Weather Forecasts (ECMWF) [3] to accurately depict how atmospheric events affect precipitation has been demonstrated. Nonetheless, many studies have shown that the outcome of a dynamic forecasting model is significantly

The associate editor coordinating the review of this manuscript and approving it for publication was Abdullah Iliyasu.

biased in various aspects when compared to real observations. Therefore, numerous bias-correction techniques have been developed to improve and localize the dynamic forecasting model's results. Due to their simplicity and explainability, statistical approaches such as statistical downscaling [4] and quantile mapping [5] have also been among the most often used methods for precipitation bias-correction for decades. Recently, however, deep learning has significantly advanced and excelled in many meteorological applications, especially convolutional neural networks (CNN) [6], [7], [8], [9]. Further studies have also been carried out concerning the impact of various meteorological variables [10], [11] on S2S precipitation. As a result, deep learning combined with meteorological effects can have a great effect on precipitation bias-correction.

Of late, interest in S2S forecasting has increased. Because of the chaotic nature of the atmosphere, it is typically thought of as a difficult time horizon to forecast. Scientific advancements combined with a better knowledge of S2S sources of predictability have resulted in notable increases in predicting skills. Numerous studies demonstrate that dynamic forecasting models such as CFSv2 [2] and ECMWF [3] are effective at forecasting meteorological variables: namely, temperature,wind, and geo-potential height. However, when predicting precipitation, dynamic forecasting models are found to be far less accurate than predicting temperature [12]. Several attempts have been made to improve S2S prediction capabilities.

In this study, we aim to correct the bias in the CFSv2 dataset with our deep-learning model. Our model is assessed over three time periods: weeks 1-2, weeks 3–4, and weeks 5–6. Our model, Attention U-Net [8], is modified to correct CFSv2 precipitation dataset bias. Multi-task learning employs a combination of customized regression loss and classification loss. Moreover, we concentrate on data preparation to lessen the influence that a CFSv2 dataset's skewness has on bias-correction tasks.

This paper's contributions are summarized as follows:

- We bias-corrected the sub-seasonal CFSv2 precipitation using an image-like deep learning network such as Attention U-Net.
- Two modules help us to improve our model. To begin with, a multi-scale residual block is employed to learn the patterns that appeared on various scales. Then, to enhance the model learning process, a combination of customized regression loss and classification loss is employed.
- We used a log scaler for scaling precipitation data to lessen the impact of the skewness of the data. The added advantage is that the range of data appears to be more linear, which helps in the process of model training.
- We also used seasonal and meteorological data to provide information about Thailand's unique precipitation patterns.

This work duly investigates precipitation bias-correction in Thailand. Numerous machine learning studies have been carried out. As yet, however, a thorough exploration of bias corrected S2S precipitation has not been undertaken. Herein, we wish to expand upon this work. Our work, therefore, is new and proves to be effective.

The rest of this paper is organized as follows: Section II discusses the related work. Section III describes the dataset and proposed method. Section IV describes the experimental settings. Section V displays the experiment's results and discussion. Section VI gives the conclusion of this paper.

II. RELATED WORK

S2S precipitation bias-correction is a challenging topic. Several approaches have been developed to address this issue. Herein, we divided our approach into two categories. The first, frequently utilized by meteorological experts is a statistical approach. The second is an ML-based technique for correcting bias in precipitation data at various time scales.

A. STATISTICAL APPROACH FOR SUB-SEASONAL TO SEASONAL PRECIPITATION BIAS-CORRECTION

Due to the potential ability of CFSv2 in predicting S2S precipitation, several methods to correct S2S precipitation bias from the dynamic forecasting system's results have been developed. In general, to correct the bias of CFSv2 precipitation, a variety of statistical techniques, including quantile mapping and statistical downscaling [4], have been used for bias-correcting CFSv2 precipitation data. Specq and Batté [13] applied a statistical-dynamic bias-correction based on a Bayesian framework corporate with El Nino Southern Oscillation (ENSO) and Madden-Julian Oscillation (MJO) as the predictors. Vigaud et. al. [14] demonstrated a spatial correction methodology for multi-model S2S precipitation forecasts using local Laplacian eigenfunctions. Li et. al. [5] determined a copula-based postprocessing method, which modified probability distribution, allowing their model to improve prediction concerning extreme values.

Linear downscaling is commonly utilized and widely acknowledged as a statistical technique [15] for correcting biases in precipitation results. In this study, we specifically adopt linear downscaling as the baseline method representing the statistical approach. The CFSv2 predictions are corrected by the linear downscaling technique utilizing monthly climatology as follows:

$$P'_{cfs_{i,j}} = P_{cfs_{i,j}} \times \frac{\mu_{obs_{i,m}}}{\mu_{cfs_{i,m}}} \tag{1}$$

where $\mu_{obs_{i,m}}$ denotes the monthly climatology of the Hydro-Informatics Institute (HII) observation at month m at the i-th position, $\mu_{cfs_{i,m}}$ denotes the monthly climatology of the CFSv2 data at month m at the i-th position, $P_{cfs_{i,j}}$ denotes the initial prediction from the CFSv2 model at the j-th sample and the i-th position. Finally, $P'_{cfs_{i,j}}$ signifies the corrected prediction from the CFSv2 model at the j-th sample and the i-th position.

B. MACHINE LEARNING-BASED PRECIPITATION BIAS-CORRECTION MODEL

Initially, precipitation bias-correction relied on some basic machine learning methods. Subsequently, numerous machine learning (ML) based studies on bias-correction precipitation at various time scales have been carried out. As yet, a thorough exploration of a deep learning (DL) model capable of bias-correcting S2S precipitation has not been undertaken. To solve this problem, deep-learning methods have recently been applied.

As such, machine-learning-based approaches i.e., random forests [16], [17], [18], [19], support vector machines [20], [21], and artificial neural networks [22], [23] have been used for bias-correction of S2S precipitation. Hwang et al. [11], for instance, used two non-linear machine-learning models to bias-correct CFSv2's precipitation and temperature data. Wang et al. [6], predicted hourly gridded precipitation using the SRDRN model with a multi-task technique. Fang's research showed much promise when using deep learning as a forecasting model. Espeholt et al. [7] employed MetNet to bias-correct and increase the resolution of precipitation from a numeric weather prediction (NWP) model. Moreover, Attention U-net architect [8] has been used on precipitation bias-correction tasks and has shown promising results. Ji et al. [9] implemented two CNN networks as a post processing method for probabilistic forecasting.

In this study, we chose Attention U-Net, a recent advancement in the bias correction of precipitation utilizing DL, to represent our ML-based precipitation bias-correction baseline. The Attention U-Net model is based on a U-Net model [24] with the addition of an attention gate (AG). In modern studies of precipitation bias-correction utilizing a deep-learning based model, U-Net architecture is frequently utilized as the base model. U-Net is a U-shaped architecture comprising an encoder and a decoder. U-Net achieves a pixel-to-pixel mapping process applied between the input and output image. As shown in Fig. 2, Attention U-Net, shown in the white blocks, added an attention gate (red blocks) between the encoder-decoder skip connection. This attention gate helps in learning a specific pattern of precipitation. However, the Attention U-Net architecture proved unsuitable for predicting strongly fluctuating precipitation patterns at various scales. Therefore, the Attention U-Net model was modified to bias-correct CFSv2 precipitation on S2S time scale.

III. METHODOLOGY

This paper proposes the modified Attention U-Net for precipitation bias-correction. This section consists of three parts: dataset, data preprocessing, and the proposed model. The first section describes in detail each dataset used in this study. Secondly, data preprocessing is used to handle precipitation data, which is a highly skewed dataset; all data has to be in the same format. Furthermore, the data processing of meteorological data and seasonal data is provided. Finally, the proposed model, which is based on the Attention U-Net model, and its modifications are explained.

TABLE 1. A summary of the dataset characteristics.

Features	Unit	Description
Precipitation		
CFSv2 precipitation	kg/m^2	A P_{rate} feature produced by the CFSv2 model.
HII precipitation	$mmHg$	Precipitation data was collected by HII from numerous stations throughout Thailand.
Meteorological indices		
MJO	-	A Madden Julian Oscillation is the most significant source of intraseasonal variability in the tropical atmosphere.
IM Index	-	An Indian Monsoon Index represents monsoon trends in the Indian Ocean.
WNPM Index	-	A Western Northern Pacific Monsoon Index represents monsoon tendencies in the Pacific Ocean around Thailand.

A. DATASET DESCRIPTION

In this study, two precipitation datasets are used. The first dataset is CFSv2, which is provided by the National Oceanic and Atmospheric Administration (NOAA). The CFSv2 data comes in NetCDF files with $0.2° \times 0.2°$ resolution. The other dataset is the daily observation data from the Hydro-Informatics Institute (HII). The HII dataset has been collected since 2012 and provides a resolution of $1km \times 1km$. Herein, we corrected the CFSv2 dataset (input) to the HII dataset (ground truth).

As precipitation is affected by meteorological events, three additional meteorological indices were collected as an indicator for those events. The first index is MJO, which is an eastward moving disturbance of clouds, rainfall, winds, and pressure that traverses the planet in the tropics and returns to its initial starting point in 30 to 60 days, on average. MJO has proved to be a significant factor in sub-seasonal precipitation forecasting; MJO is provided by the Australia's bureau of meteorology (BOM). The second index is the Indian Monsoon (IM), which is the most prominent of the world's monsoon systems that affects India and its surrounding areas, including Thailand. The Indian monsoon blows from the northeast during cooler months and reverses direction to blow from the southwest during the warmest months of the year. This process brings large amounts of rainfall to the region during June and July. The Indian monsoon index is provided by NOAA. The Western Northern Pacific Monsoon (WNPM) index is the last index in this study, which is a part of the intertropical convergence zone in the western northern Pacific Ocean and has an impact on the eastern region of Thailand. The WNPM index is provided by NOAA.

In summary, this study utilized two aspects of data, which are precipitation and three meteorological indices. In Table 1, a summary of dataset characteristics is given.

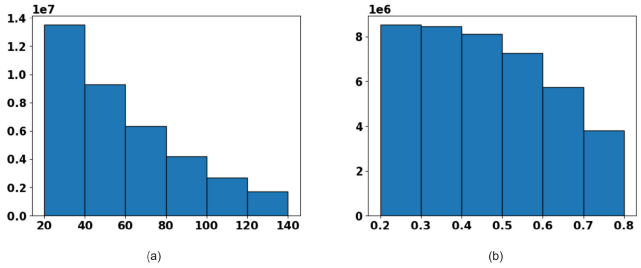

FIGURE 1. Two histograms of the dataset distribution: (a) HII's raw dataset distribution, and (b) HII's dataset distribution after using a log scaler.

B. DATA PREPROCESSING

This section is divided into two parts: the preprocessing of precipitation data and the preprocessing of meteorological indices. The precipitation preprocessing section discusses how to construct a uniformly formatted dataset and scaling approach. Later, the preprocessing of meteorological indices demonstrates how each index has been processed and summarized for the model's input.

1) PRECIPITATION DATA

The objective of preprocessing is to create a uniform format that can combine together all the information from each source. Preprocessing of precipitation data consists of two processes: re-grid precipitation data and scaling data.

The difference in resolution between the precipitation datasets requires the process of re-gridding. To match the increased resolution of the HII dataset, the CFSv2 dataset must be modified. CFSv2 dataset was chosen from the 5.0° to 13.0° latitude and from 97.0° to 105.0° longitude. Following that, the selected CFSv2 data was interpolated using the invert distance weight (IDW) method to scale the CFSv2 resolution to meet HII resolution.

After re-gridding the precipitation data, one issue remains, which is the skewness of the data. Precipitation fluctuation produces a wide range of precipitation data and a non-uniform distribution of precipitation data. This makes training the model difficult. Therefore, we utilized a log scaling method, which is defined as follows, to reduce the effect of the data skewness:

$$X' = log_{10}(X/\alpha + 1) \tag{2}$$

where X' denotes the scaled precipitation value and X denotes the original precipitation value; α is a scaling factor that controls the range of X' being mostly between 0 and 1. Compared to raw precipitation data, the log scaled precipitation data appear to be distributed more uniformly, as shown in Figure 1.

Precipitation preprocessing enables CFSv2 to have the same resolution as HII data, which makes it easier to use the existing deep-learning models. In addition, log scaling improves the learning process and reduces the exploding gradient problem.

2) METEOROLOGICAL INDICES AND SEASONAL DATA

The MJO, WNPM index, and IM index are the meteorological indices that are used in this study. The MJO index is made up of three elements of information: RMM1, RMM2, and phase. Thus, MJO is expressed as:

$$MJO_{rep} = (RMM1^2 + RMM2^2) \times phase \tag{3}$$

$RMM1$ and $RMM2$ are amplitudes of the first and second elements of the MJO, respectively, since MJO is produced using a signal processing technique. A phase of the index is represented by the variable *phase*, and each phase affects a certain area of the globe. Hence, all meteorological indices and MJO representations are scaled using a min-max scaler; summarized values for each index and each week of the year are determined.

Seasonal data is used to provide the model with historical trends. We used data obtained from the same week of year of the previous year as our seasonal data for this study. This provides an understanding about how the historical pattern is developed.

Following the completion of data preprocessing, the data was divided into three datasets for each prediction horizon. Such details can be found in Section IV of this paper. Each dataset uses CFSv2 prediction as an input and the timely HII data that corresponds to it as a ground truth for the model. Further, the model was given additional information in the form of seasonal data and summarized indices for the past eight weeks of each prediction time.

C. ATTENTION U-NET WITH MULTI-TASK HEAD

The Attention U-Net model serves as the base for the proposed modified Attention U-Net model. Since precipitation patterns fluctuate greatly, it is challenging for a deep-learning algorithm to learn these patterns. Attention gate helps with the learning of precipitation patterns. The attention mechanism can locate the precipitation areas. As such, the attention coefficient values in these areas will be large. In contrast, the attention coefficient of other areas will be close to 0. Attention gate is a 2-D attention module that suppresses feature activation in irrelevant regions while focusing on specific regions. An additive attention mechanism is used in the attention gate. Due to its lightweight construction, the attention gate significantly improves the model's ability to represent data without increasing computational costs or the number of model parameters. As shown in Fig. 2, the modified Attention U-Net model, using the two additional modules: multi-scale residual block, and multi-tasking, is implemented.

When a high-resolution image is bias-corrected, the precipitation patterns have different scales. To handle patterns on various scales, Attention U-Net architecture makes use of max-pooling layers. However, this may result in the loss of information. The multi-scale residual block implements three residual blocks with kernel sizes of 5, 7, and 9. The purpose of this module is to identify patterns across three different scales to provide high-resolution prediction.

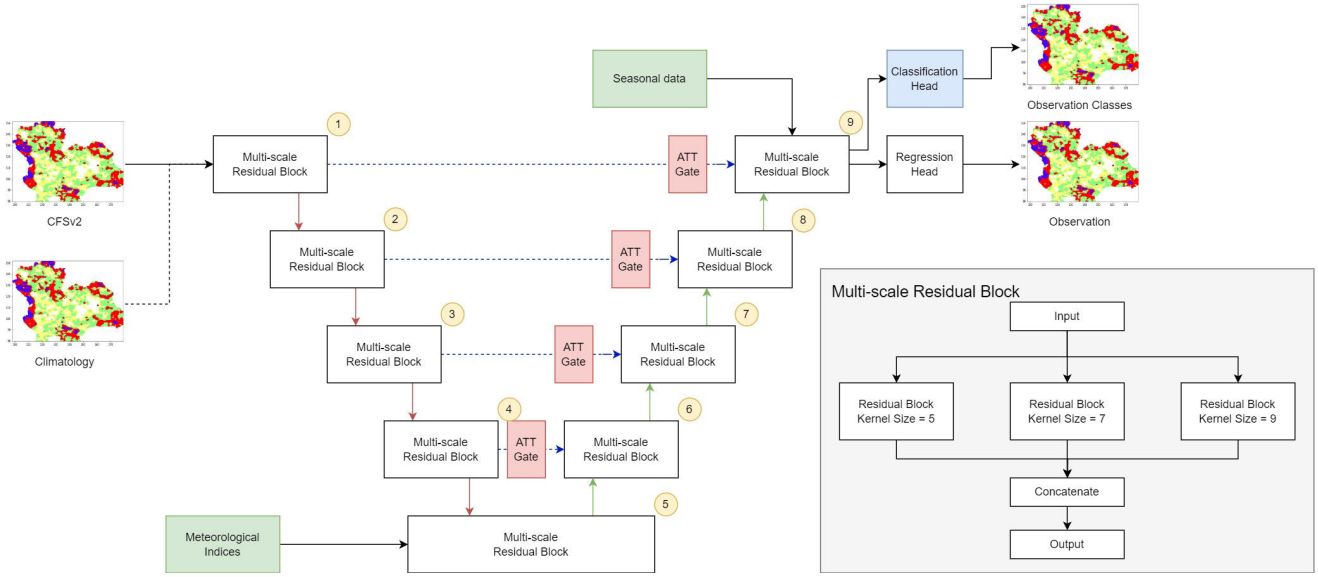

FIGURE 2. Schema of the modified Attention U-Net architecture (four modules): (1) The white blocks show the multi-scale residual blocks implemented based on U-Net architecture, (2) The red blocks show how we use "Attention Gate" in our model, (3) The blue block represents the multi-tasking module, and (4) The green blocks represent the use of meteorological indices and seasonal data in our model.

Our dataset has a high degree of skewness, making it difficult for traditional learning techniques to reliably predict the range of precipitation. In predicting extreme precipitation events, the classification head is used with a focal loss to help the model. Moreover, our model input includes seasonal data and meteorological indices. Each module aids the model in enhancing its functionality while preserving and learning from the historical pattern at its highest resolution. It is noted that our model uses a multi-head design to support multi-task learning. Our loss is a combination of regression and classification loss, as defined below:

$$Loss = \beta_1 \cdot RL + \beta_2 \cdot CL \tag{4}$$

where β_1 and β_2 denote a scaling factor for regression loss and classification loss, respectively. RL and CL stand for regression loss and classification loss, respectively. β_1 and β_2 are used to scale two losses so that the model can learn equally from both the regression head and the classification head. Initial ranges for the classification loss and regression loss are (0 to 1) and (0 to 0.1), respectively. As a result, we use β_1 and β_2 equal to 1.2 and 0.1 so that our regression and classification losses are in the same magnitude.

In the regression aspect, we applied customized loss to help the model anticipate the occurrence of rain by penalizing the raining grid more severely. We also modified the weight component of the weighted mean absolute error (MAE), which is written as:

$$RL = \frac{\sum_{i=1}^{n} w_i \times \left| y_{pred} - y_{true} \right|}{n} \tag{5}$$

$$w_i = \begin{cases} min & y_{true} \leq \min \\ y_{true} & min < y_{true} \leq \max \\ max & y_{true} > max \end{cases} \tag{6}$$

where w is the weight of each grid, y_{true} is the log-scaled HII's precipitation, y_{pred} is the log-scaled CFSv2's precipitation, n is the number of grids, and min and max denotes the minimum and maximum weight value. In this study, we use min equals to $\log(10/\alpha + 1)$ and max equals to $\log(100/\alpha + 1)$, which is the minimum and maximum criteria of precipitation as defined by the Thai meteorological department (TMD). α is a scaling factor to scale precipitation values to be less than 1. In this study, we use α equals to 20. Customized regression loss aids in the model's ability to identify patterns in the imbalanced dataset by imposing a greater penalty when it is raining than when it is not.

In the classification head, we used focal loss [25] to handle the problem of class imbalance, as our classification loss. The goal of focal loss is to increase the loss of the class with fewer members while decreasing the loss from the class with greater members. Our classification loss is defined as:

$$CL = -(1 - p_t)^{\gamma} log(p_t) \tag{7}$$

where p_t denotes the class's estimated probability predicted by the model. γ is tunable parameter called the focusing parameter. In this study, we chose to use γ equals to 4 using the grid search technique.

IV. EXPERIMENTAL SETTING

A. HARDWARE AND SOFTWARE SPECIFICATION

In this work, we used TensorFlow 2.0 and Python 3.8.3 to train our models. The training device is set up with a NVIDIA 3070 graphics card and 24 GB of RAM.

B. DATASET

The data used in the study was collected between the years: 2012 and 2020. The years 2012 to 2017 were selected as our

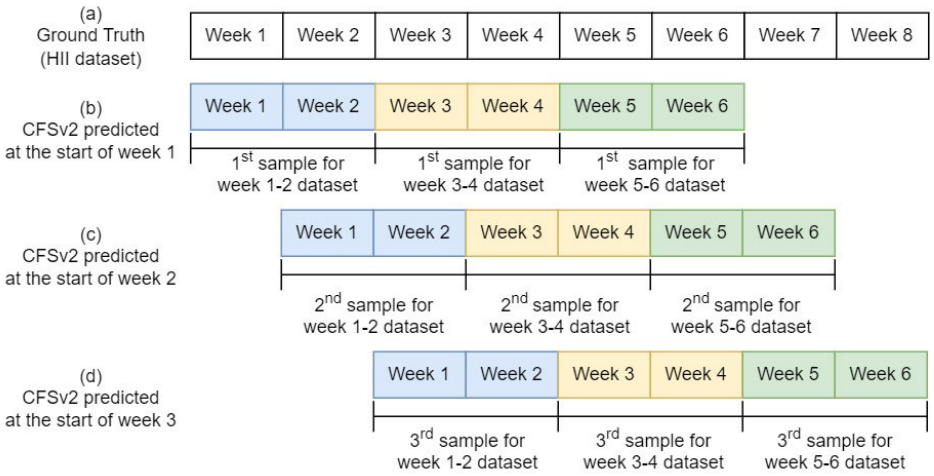

FIGURE 3. Schematic diagram for preparation of dataset: (a) The ground truth shows HII's precipitation dataset, which is collected continuously, (b) CFSv2 dataset is produced weekly showing how CFSv2 dataset produced at the start of the 1st week has been handled. Both (c) and (d) demonstrate how we handle CFSv2 dataset produced at the start of the 2nd and 3rd week, respectively.

training set. The year 2018 was selected as our validation set. Our test set involved the years 2019 and 2020. This choice was chosen to hold onto data patterns that happen annually. As shown in Fig. 3, we used 6 weeks of CFSv2 predictions, which were predicted at the start of each week, for each of the samples. We divided the 6 weeks of forecast data into 3 periods: Weeks 1-2, Weeks 3–4, and Weeks 5–6. Following the collection of three datasets for each prediction horizon, the associated observation data were chosen as the ground truth for each model. Finally, our results are evaluated on the testing dataset.

C. MODEL DETAILS

The modified Attention U-Net architecture, as depicted in Fig. 2, contains a total of nine layers of multi-scale residual blocks. The multi-scale residual block consists of three residual blocks, each utilizing a kernel size of 5, 7, and 9, respectively. The ELU activation function is employed in this setting. According to the diagram, layers of the same size are configured in a similar setting. Residual blocks in layers 1 and 9 are equipped with a total of four filters. Each residual block in layers 2 and 8 consists of 8 filters. In each residual block, there are 16 filters allocated for both layers 3 and 7. The residual blocks in layers 4, 5, and 6 consist of 32 filters.

In terms of model complexity, our model has 1.2 million trainable parameters based on the configuration mentioned in previous paragraph. The baseline model, Attention U-Net with residual blocks and a kernel size of 7, has 500 thousand trainable parameters in total. Our model's complexity exceeds that of the Attention U-Net model.

D. TRAINING SETTING

During the training process, the ADAM optimizer was employed as the chosen optimization algorithm. The learning rate configuration for the ADAM optimizer was set at 0.01, while the values of β_1 and β_2 were set as 0.9 and 0.999, respectively. In terms of the loss function, a combined loss was employed in the training process. The loss expressions are specified in equations 4, 5, 6, and 7 respectively.

E. EVALUATION CRITERIA

This paper evaluated the model's performance in two different ways. The first aspect focused on the regression aspect, which evaluates the results directly from our model. Herein, the study used the root mean square error (RMSE) to evaluate performance. RMSE is defined as follows:

$$RMSE = \sqrt{\frac{1}{n}\sum_{i=1}^{n}\left(Y_i - \hat{Y}\right)^2} \tag{8}$$

where n is the number of samples in the test dataset, Y_i is the i-th ground truth, and $\hat{Y}$ is the i-th prediction.

The second aspect of our study involved the correlation of our model. We used the temporal correlation coefficient (TCC), which is a Pearson correlation coefficient for each grid across all test datasets. TCC can be expressed as:

$$TCC = \frac{\sum_{i=1}^{n}\left(\hat{Y}_i - \hat{\mu}\right)(Y_i - \mu)}{\sqrt{\sum_{i=1}^{n}\left(\hat{Y}_i - \hat{\mu}\right)^2 \sum_{i=1}^{n}(Y_i - \mu)^2}} \tag{9}$$

where n is the number of samples in the test dataset, Y_i is the i-th ground truth, $\hat{Y}$ is the i-th prediction, $\hat{\mu}$ is the mean of $\hat{Y}$ at each grid, and μ is the mean of Y at each grid.

V. RESULTS AND DISCUSSIONS

In this section, we aim to show the results, analyses, and discussions of our model compared to all baselines on the testing dataset. There are three subsections. First, it aims to illustrate the overall performance comparison. Second, the ablation study is reported to provide an effect of

each proposed module. Finally, the discussion is presented focusing on two aspects: (1) the result during a tropical storm period and (2) a spatial evaluation.

Our proposed model is based on the Attention U-Net architecture. The multi-scale residual blocks, multitask learning, and the use of meteorological indices are the three proposed improvements in this work that are examined in the ablation test. As shown in Table 2, all results described in the next sections will have five feature-related acronyms.

TABLE 2. Acronyms of our proposed features.

Acronym	Description
LD	Linear downscaling technique
ATT-UNET	Attention U-Net model
MS	The inclusion of the multi-scale residual blocks
MT	The inclusion of multi-task learning with customized regression loss and focal loss
ME	The inclusion of meteorological indices and seasonal effects

S2S forecasting is related to a prediction of 2-6 weeks in advance, and different regions (e.g., northern and southern of Thailand) often have different precipitation characteristics. Thus, in all following subsections, the evaluation results are always reported in details of two aspects: time periods (1-2 weeks, 3-4 weeks, and 5-6 weeks) and regions (overall, northern, and southern).

A. OVERALL PERFORMANCE

In this subsection, Table 3 was presented to show an overall performance of our model (ATT-UNET-MS-MET-ME) and two baselines (LD and ATT-UNET). There are two evaluation measures: the root mean square error (RMSE) and the temporal correlation coefficient (TCC).

For the overall time horizons, Table 3 shows that our model outperformed LD and ATT-UNET for 8.65% and 15.56% in terms of RMSE improvements and 13.77% and 12.06% in terms of TCC improvements. Moreover, it shows the same results that our model is also the winner for northern and southern areas.

For the details of each time horizon, Table 3 shows that our model is superior to both baselines in all time horizons (1)-2, 3-4, and 5-6 weeks). In the 1 to 2 week horizon, we reached 24.80 mmHg in RMSE and 0.62 in TCC. Furthermore, the 3 to 4 week results established RMSE of 24.74 mmHg and TCC of 0.63. Finally, the 5 to 6 week horizon's RMSE proved to be 23.30 mmHg and TCC reached 0.65.

In Fig. 4, our model (green line) outperforms other baselines, exhibiting the lowest RMSE across all regions. Notably, a favorable downward trend in RMSE can be observed as the time horizon extends. The LD model (blue line) maintains a consistent level of statistical accuracy with a stable RMSE across all time horizons. However, the ATT-UNET model shows suboptimal performance, particularly in the 1 to 2-week horizon, where its RMSE surpasses all other models.

TABLE 3. The model's performance for years: 2019 and 2020 is shown with the RMSE and TCC for each region and prediction horizon. Boldface refers to the winners. The values in brackets refer to the improvement in percentage over LD (first value) and ATT-UNET (second value).

Metrices		LD	ATT-UNET	ATT-UNET-MS-MT-ME (ours)
Average of all time horizons				
Overall	**RMSE↓**	26.58	28.75	**24.28** (+8.65%,+15.56%)
	TCC↑	0.56	0.57	**0.63** (+13.77%,+12.06%)
Northern	**RMSE↓**	22.93	25.27	**21.21** (+7.50%,+16.07%)
	TCC↑	0.59	0.62	**0.67** (+13.56%,+8.74%)
Southern	**RMSE↓**	43.39	44.81	**38.44** (+11.42%,+14.23%)
	TCC↑	0.43	0.33	**0.47** (+8.46%,+42.44%)
Details of each time horizon (1-2, 3-4, 5-6 weeks)				
Week 1-2				
Overall	**RMSE↓**	26.86	32.21	**24.80** (+7.67%,+23.01%)
	TCC↑	0.55	0.57	**0.62** (+12.73%,+9.68%)
Northern	**RMSE↓**	22.97	30.12	**21.57** (+6.09%,+28.39%)
	TCC↑	0.59	0.61	**0.66** (+11.86%,+8.25%)
Southern	**RMSE↓**	44.79	41.84	**39.69** (+11.39%,+5.14%)
	TCC↑	0.41	0.36	**0.42** (+2.44%,+16.50%)
Week 3-4				
Overall	**RMSE↓**	26.36	26.66	**24.74** (+6.15%,+7.19%)
	TCC↑	0.56	0.57	**0.63** (+12.50%,+9.59%)
Northern	**RMSE↓**	22.81	22.35	**21.55** (+5.52%,+3.59%)
	TCC↑	0.59	0.64	**0.67** (+13.56%,+5.47%)
Southern	**RMSE↓**	42.72	46.51	**39.45** (+7.65%,+15.17%)
	TCC↑	0.44	0.30	**0.48** (+9.09%,+61.92%)
Week 5-6				
Overall	**RMSE↓**	26.52	27.39	**23.30** (+12.14%,+14.94%)
	TCC↑	0.56	0.56	**0.65** (+16.07%,+17.04%)
Northern	**RMSE↓**	23.01	23.34	**20.51** (+10.86%,+12.12%)
	TCC↑	0.59	0.60	**0.68** (+15.25%,+12.66%)
Southern	**RMSE↓**	42.66	46.10	**36.17** (+15.21%,+21.53%)
	TCC↑	0.45	0.33	**0.51** (+13.33%,+53.17%)

As previously stated, the results show that our model outperformed both the statistical and machine learning-based baseline models in every respect. To highlight the progress accomplished, it is worth noting that our model demonstrated considerable improvements in Thailand's southern region, which is regarded as the most fluctuating region due to the occurrence of storms throughout the year.

B. ABLATION TEST

In addition to the overall performance evaluation, we conduct a feature ablation test outlined in Table 4. The table presents six models, each featuring distinct combinations of attributes. The initial model, ATT-UNET, implements the Attention U-Net model. The second model, ATT-UNET-MS, is a variation of ATT-UNET, integrating multi-scale residual blocks. The third model, ATT-UNET-MT, employs a multi-task learning technique with a customized loss for the regression head and a focal loss for the classification head. The fourth model, ATT-UNET-ME, introduces meteorological indices and seasonality effect as additional information for the ATT-UNET model. The fifth model, ATT-UNET-MS-MT, combines ATT-UNET with multi-scale residual blocks and

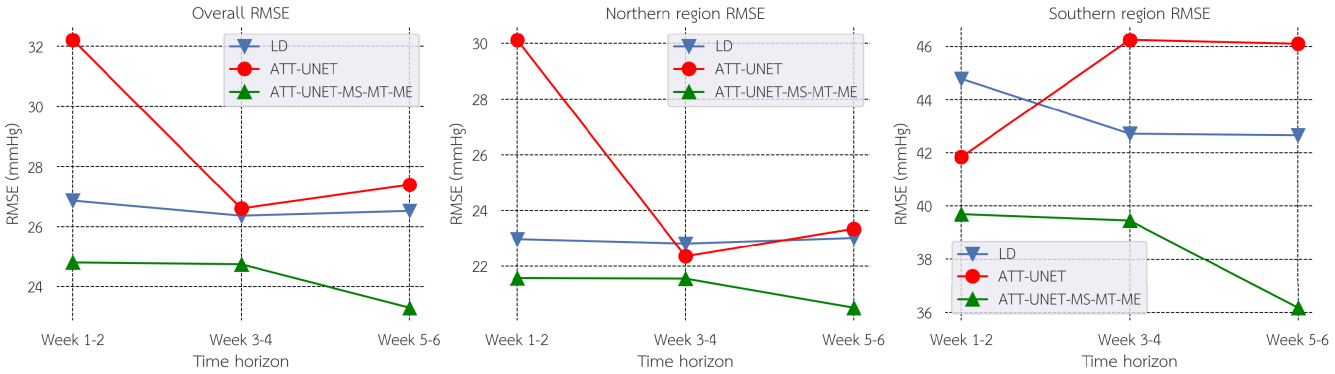

FIGURE 4. RMSE comparison between Linear downscaling technique (blue line), ATT-UNET (red line), and ATT-UNET-MS-MT-ME (green line). The left graph is the overall RMSE comparison. The middle graph is the RMSE comparison in the northern region. Finally, the right graph is the RMSE comparison in the southern region. In each graph, the vertical axis represents the RMSE in mmHg. the horizontal axis represents the time horizon.

TABLE 4. Features ablation study in terms of RMSE and TCC for each prediction horizon and region. Numbers with % refer to the improvement in percentage over the ATT-UNET model. Boldface refers to the winners. The green numbers indicate the improvement of our model over U-Net model while red numbers indicate no improvement.

Metrices		ATT-UNET	ATT-UNET-MS		ATT-UNET-MT		ATT-UNET-ME		ATT-UNET-MS-MT		ATT-UNET-MS-MT-ME (ours)	
Average of all time horizons												
Overall	**RMSE↓**	28.75	26.07	+8.52%	28.37	+0.86%	25.52	+10.63%	25.70	+9.94%	**24.28**	+15.05%
	TCC↑	0.57	0.60	+6.77%	0.59	+3.85%	0.58	+2.04%	**0.63**	+12.11%	**0.63**	+12.11%
Northern	**RMSE↓**	25.27	23.37	+5.57%	25.16	-0.91%	22.88	+7.86%	21.85	+11.76%	**21.21**	+14.70%
	TCC↑	0.62	0.64	+4.45%	0.64	+3.94%	0.61	-1.33%	**0.68**	+10.41%	0.67	+8.79%
Southern	**RMSE↓**	44.81	38.54	+13.83%	43.15	+3.45%	**37.65**	+15.80%	43.49	+2.55%	38.44	+13.95%
	TCC↑	0.33	0.42	+27.03%	0.34	+4.03%	0.43	+32.44%	0.42	+29.32%	**0.47**	+43.86%
Details of each time horizon (1-2, 3-4, 5-6 weeks)												
Week 1-2												
Overall	**RMSE↓**	32.21	25.43	+21.05%	29.61	+8.09%	25.50	+20.83%	25.50	+20.83%	**24.80**	+23.01%
	TCC↑	0.57	0.60	+6.14%	0.58	+2.18%	0.57	0%	**0.62**	+9.68%	**0.62**	+9.68%
Northern	**RMSE↓**	30.12	22.70	+24.64%	26.58	+11.76%	22.91	+23.94%	**21.04**	+30.15%	21.57	+28.39%
	TCC↑	0.61	0.63	+3.33%	0.64	+5.09%	0.61	0%	**0.68**	+11.53%	0.66	+8.25%
Southern	**RMSE↓**	41.84	38.02	+9.13%	43.56	-4.11%	**37.44**	+10.51%	46.05	-10.06%	39.69	+5.14%
	TCC↑	0.36	**0.43**	+19.28%	0.28	-21.01%	0.42	+17.09%	0.36	-0.14%	0.42	+16.50%
Week 3-4												
Overall	**RMSE↓**	26.66	27.61	-3.58%	29.03	-8.91%	25.61	+3.91%	25.82	+3.14%	**24.74**	+7.19%
	TCC↑	0.57	0.61	+6.11%	0.57	0%	0.57	0%	**0.63**	+9.59%	**0.63**	+9.59%
Northern	**RMSE↓**	22.35	25.23	-12.88%	26.17	-17.09%	23.10	-3.36%	21.97	+1.71%	**21.55**	+3.59%
	TCC↑	0.64	0.65	+2.32%	0.62	-2.22%	0.60	-5.39%	**0.68**	+7.05%	0.67	+5.47%
Southern	**RMSE↓**	46.51	38.57	+17.06%	42.22	+9.21%	**37.20**	+20.02%	43.61	+6.23%	39.45	+15.17%
	TCC↑	0.30	0.42	+41.68%	0.33	+11.28%	0.45	+51.17%	0.40	+34.94%	**0.48**	+61.92%
Week 5-6												
Overall	**RMSE↓**	27.39	25.18	+8.08%	26.46	+3.39%	25.43	+7.15%	25.79	+5.85%	**23.30**	+14.94%
	TCC↑	0.56	0.60	+8.04%	0.61	+10.33%	0.58	+4.95%	**0.65**	+17.04%	**0.65**	+17.04%
Northern	**RMSE↓**	23.34	22.18	+4.96%	22.73	+2.60%	22.64	+2.99%	22.54	+3.42%	**20.51**	+12.12%
	TCC↑	0.60	0.65	+7.69%	0.66	+8.94%	0.62	+2.05%	**0.68**	+12.66%	**0.68**	+12.66%
Southern	**RMSE↓**	46.10	39.04	+15.31%	43.67	+5.26%	38.32	+16.87%	40.80	+11.49%	**36.17**	+21.53%
	TCC↑	0.33	0.40	+20.13	0.41	+21.84%	0.43	+29.07%	**0.51**	+53.17	**0.51**	+53.17%

multi-task learning. The final model, ATT-UNET-MS-MT-ME, incorporates all these strategies.

On the average of three time horizons, overall, our model, ATT-UNET-MS-MT-ME, with all its features, is seen to be the winner model with the RMSE of 24.28 mmHg and TCC of 0.63. In the northern region, the ATT-UNET-MS-MT-ME emerges as the winner in terms of RMSE, with a value of 21.21 mmHg. The ATT-UNET-MS-MT model achieves a TCC value of 0.68, which closely matches the TCC value of ATT-UNET-MS-MT-ME in the northern region.

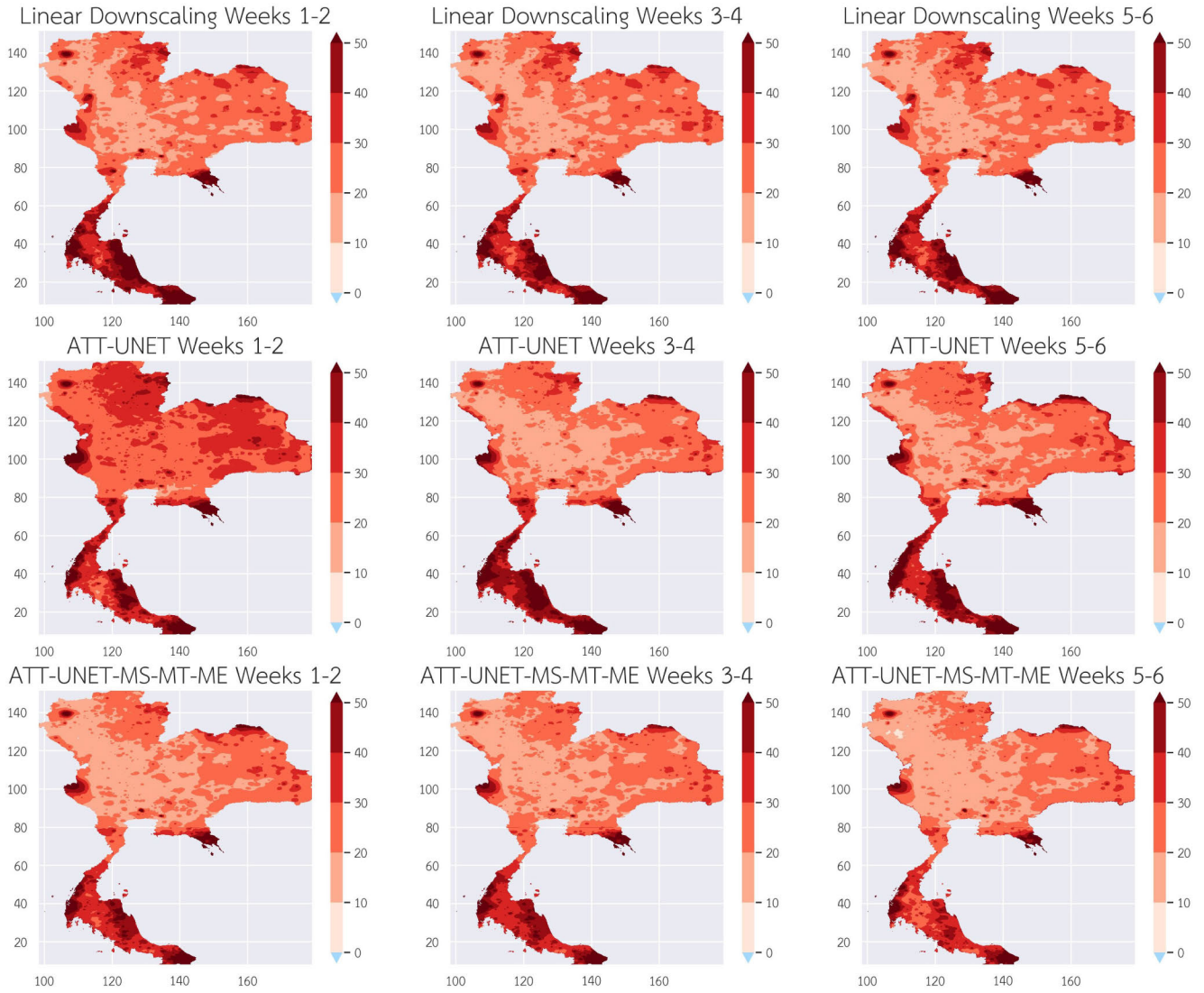

FIGURE 5. RMSE comparison between Linear downscaling technique (first row), ATT-UNET (second row), and ATT-UNET-MS-MT-ME (third row). The first column is the comparison from week 1 to 2 model. The second column is the comparison from week 3 to 4 model. Finally the last column is comparison from week 5 to 6 model. In each figure, the high RMSE value grids appear in dark red.

In the southern region, the model ATT-UNET-MS-MT-ME has outstanding results in both evaluated aspects, with a RMSE of 38.44 mmHg and a TCC of 0.47.

The ablation study demonstrates that the addition of multi-scale residual blocks resulted in a significant improvement in RMSE over the ATT-UNET model. While multi-tasking provides minor improvements to TCC. Furthermore, the incorporation of meteorological indices led to a small boost in RMSE as well. The use of multi-tasking with a multi-scale residual block helps the model to perform better in the northern region, resulting in a significant improvement in TCC. The impact of meteorological indices on precipitation in Thailand has been investigated in a previous study [26]. As in Table 4 demonstrated, the addition of seasonal affect and meteorological indices led to substantial enhancements in the RMSE and TCC in every region. Seasonal effects can improve bias-correction similar to the seasonal effects in time-series models. While the ATT-UNET-MS-MT-ME model may not be a winner in every evaluation when breakdown to each time horizon, the findings still indicate that incorporating all features significantly improved the model's performance, surpassing baseline model.

C. DISCUSSION

1) PERFORMANCE DURING TROPICAL STORM PERIODS

Thailand frequently experiences tropical storms due to the influence of nearby monsoon systems. Table 5 is presented in this subsection to highlight how our model and baseline models performed during the tropical storm period. Our objective is to offer a more comprehensive assessment of the impact of meteorological indices. The Thai Meteorological

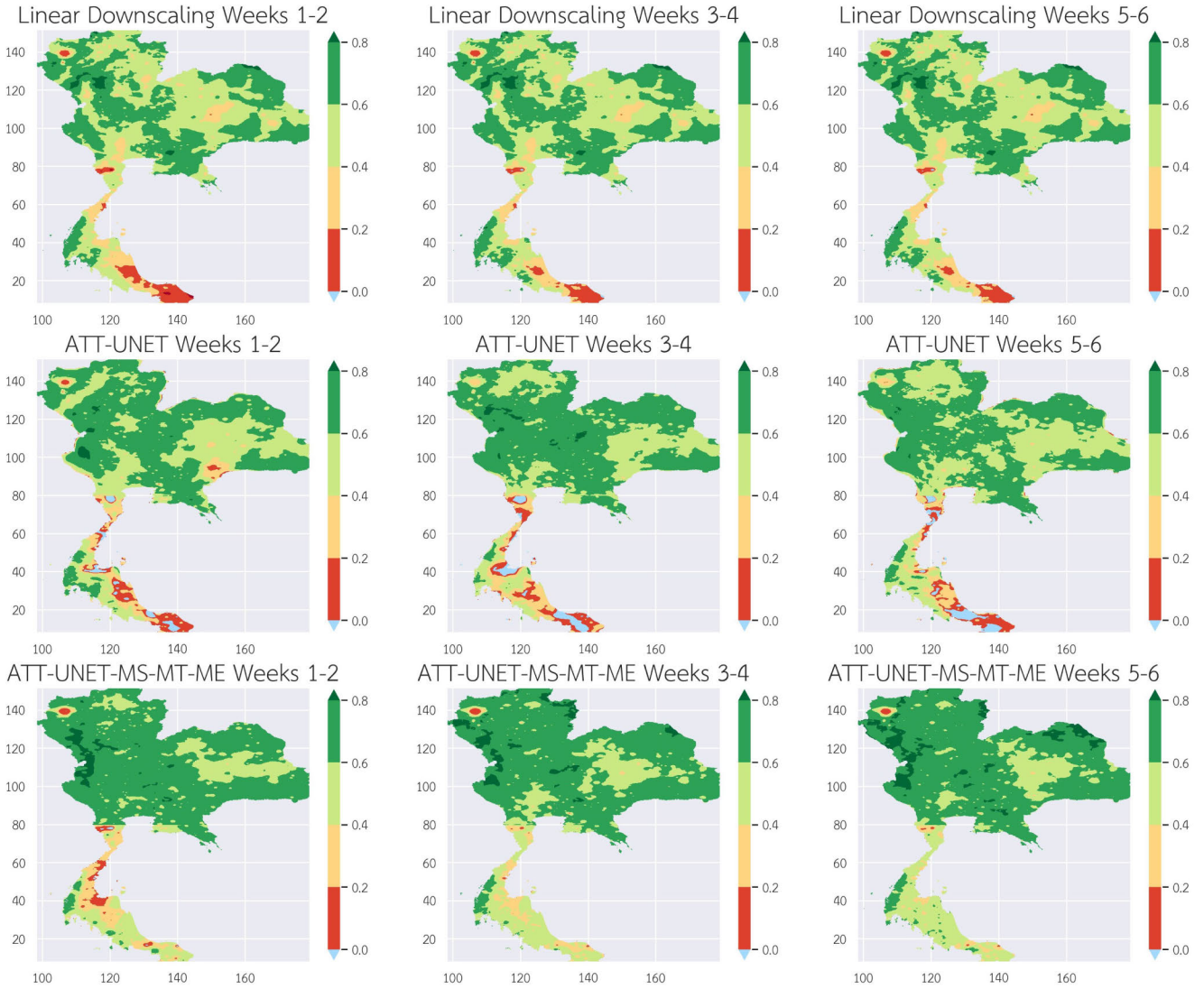

FIGURE 6. TCC comparison between Linear downscaling model (first row), ATT-UNET (second row), and ATT-UNET-MS-MT-ME (third row). The first column is the comparison from week 1 to 2 model. The second column is the comparison from week 3 to 4 model. Finally the last column is comparison from week 5 to 6 model. In each figure, the high TCC value grids appear as a green grid while the red grids represent the low TCC value grid.

Department (TMD) issues reports specifying the occurrence of tropical storms, and for this evaluation, these reports are used for selecting samples from the test dataset. Two evaluation metrics, namely RMSE and TCC, are employed to evaluate performance.

Averaging across all time horizons, Table 5 shows that our model outperformed LD and ATT-UNET by 15.43% and 14.12% in terms of RMSE improvements and 20.01% and 15.38% in terms of TCC, respectively. Furthermore, it indicates that our model is superior in both the northern and southern regions. In addition, significant improvements can be seen in the southern region, as shown by RMSE reductions of 28.76% and 11.54% when compared to LD and ATT-UNET, respectively. Moreover, when it comes to TCC in the southern region, our model outperforms LD and ATT-UNET by 32.25% and 58.40%, respectively.

The occurrence of a tropical storm leads to fluctuations in precipitation patterns, which reduces prediction accuracy. The outcome of this experiment indicates that utilizing our model with meteorological indices improves the accuracy of forecasts during storm periods. This improvement could have a positive impact on disaster planning and agricultural applications.

2) SPATIAL EVALUATION

For spatial evaluation, our aim is to see how efficiently the model worked. Spatial evaluation demonstrates the effectiveness of our model. By displaying RMSE and TCC onto a map of Thailand, we can use visualization to compare our results to the baseline models. In Fig. 5, a map representation of RMSE is shown. The dark red grid means that the RMSE of that grid is greater (worse) than the

TABLE 5. The model's performance during the tropical storm period present RMSE and TCC values for each prediction horizon and region. Boldface refers to the winners. The values in brackets refer to the improvement in percentage over LD (first value) and ATT-UNET (second value).

Metrices		LD	ATT-UNET	ATT-UNET-MS-MT-ME (ours)
Average of all time horizons				
Overall	**RMSE↓**	32.31	31.81	**27.32** (+15.43%,+14.12%)
	TCC↑	0.54	0.56	**0.65** (+20.01%,+15.38%)
Northern	**RMSE↓**	27.44	29.15	**24.79** (+9.66%,+14.96%)
	TCC↑	0.57	0.61	**0.68** (+18.28%,+10.64%)
Southern	**RMSE↓**	54.74	44.08	**39.00** (+28.76%,+11.54%)
	TCC↑	0.37	0.31	**0.49** (+32.25%,+58.40%)
Details of each time horizon (1-2, 3-4, 5-6 weeks)				
Week 1-2				
Overall	**RMSE↓**	32.24	34.40	**27.64** (+14.27%,+19.66%)
	TCC↑	0.54	0.57	**0.63** (+17.12%,+11.01%)
Northern	**RMSE↓**	26.93	32.47	**24.94** (+7.37%,+23.18%)
	TCC↑	0.58	0.62	**0.67** (+15.20%,+7.07%)
Southern	**RMSE↓**	56.71	43.29	**40.04** (+29.39%,+7.50%)
	TCC↑	0.34	0.30	**0.45** (+32.17%,+48.36%)
Week 3-4				
Overall	**RMSE↓**	32.34	30.01	**28.27** (+12.59%,+5.80%)
	TCC↑	0.54	0.57	**0.64** (+18.04%,+12.10%)
Northern	**RMSE↓**	27.70	26.71	**25.70** (+7.23%,+3.79%)
	TCC↑	0.57	0.63	**0.67** (+17.23%,+5.94%)
Southern	**RMSE↓**	53.75	45.24	**40.14** (+25.32%,+11.27%)
	TCC↑	0.39	0.27	**0.48** (+23.53%,+78.88%)
Week 5-6				
Overall	**RMSE↓**	32.34	31.03	**26.06** (+19.41%,+16.02%)
	TCC↑	0.54	0.55	**0.67** (+24.86%,+23.33%)
Northern	**RMSE↓**	27.70	28.28	**23.73** (+14.32%,+16.08%)
	TCC↑	0.57	0.59	**0.70** (+22.46%,+19.53%)
Southern	**RMSE↓**	53.75	43.72	**36.80** (+31.53%,+15.82%)
	TCC↑	0.39	0.36	**0.55** (+41.04%,+51.58%)

RMSE of a lighter red grid. Overall, our model (third row) appears to have less dark red grids, which highlight the decrease in RMSE over Thailand compared to both the linear downscaling (first row) technique and the ATT-UNET (second row) model. The northern area of Thailand has seen great improvements over the linear downscaling technique and ATT-UNET, as there are less dark red grids. Furthermore, the southern region's RMSE drastically improved over the ATT-UNET model. The southern area in the third row appears in lighter red than the southern area in the second row.

In Fig. 6, a map representation of TCC is shown. Thus, the green grid represents a high TCC value and red grid shows a low TCC value. Our model (third row) clearly outperforms both the linear-downscaling (first row) technique and the ATT-UNET (second row) model, as indicated by the greater number of green grids. In the northern region, TCC is drastically improved, outperforming both baseline models: as the map of our model's TCC is almost covered in the dark green grids. In the southern region, our model's TCC shows a competitive result with linear-downscaling technique, as our model has less red grids but also has less dark green grids as well. A significant improvement over the ATT-UNET model can be seen in the southern area since there are much less red grids.

TABLE 6. The ratio in percentage for the number of grids within each TCC range to the total number of grids. The TCC value shows the correlation between the result and the ground truth. The winning model is shown by its ability to predict a significant amount of grids with TCC values greater than 0.5, as displayed in the last column. Boldface refers to the winners and star refers to second place.

Models	TCC range (%)			
	-1.0-0.0	0.0-0.2	0.2-0.5	0.5-1.0
Week 1-2				
LD	0.17	3.54	24.98	71.31
ATT-UNET	1.54	4.15	16.68	77.63
ATT-UNET-MS	0.55	1.51	12.50	**85.43**
ATT-UNET-MS-MT	0.90	2.88	11.64	84.56
ATT-UNET-MS-MT-ME	0.14	1.76	12.72	85.38*
Week 3-4				
LD	0.06	2.63	24.40	72.92
ATT-UNET	2.16	3.93	12.12	81.75
ATT-UNET-MS	0.58	2.04	14.65	82.72
ATT-UNET-MS-MT	0.41	1.84	11.36	**86.36**
ATT-UNET-MS-MT-ME	0.04	0.40	13.65	85.90*
Week 5-6				
LD	0.05	2.53	25.22	72.20
ATT-UNET	2.34	3.58	14.54	79.38
ATT-UNET-MS	0.37	2.13	14.60	82.76
ATT-UNET-MS-MT	0.10	0.54	9.11	**90.23**
ATT-UNET-MS-MT-ME	0.04	0.36	10.25	89.31*

The table presented in Table 6 displays the count of grids within TCC range for each model. The findings indicate that the ATT-UNET-MS-MT-ME model outperformed the baseline models. Specifically, the percentage of grids falling within the high TCC range of 0.5-1.0 was 85.38%, 85.90%, and 89.31% for week 1-2, week 3-4, and week 5-6, respectively. The observed increase in the proportion of grids with TCC values over 0.5 was notable, rising from approximately 70% when employing the linear downscaling technique to approximately 80% when utilizing ATT-UNET-MS-MT-ME. While ATT-UNET-MS-MT-ME did not emerge as the winner model, it was identified as the second-best model across all three horizons. Besides, there is a slight difference between the percentage of grids in the ATT-UNET-MS-MT-ME model and the winner model that have TCC values greater than 0.5.

VI. CONCLUSION

In this paper, the modified Attention U-Net model, ATT-UNET-MS-MT-ME, was proposed and utilized in this study to correct the bias in S2S precipitation from the CFSv2 dataset. This model, based on the Attention U-Net model, included multi-scale residual blocks and multi-tasking to emphasize the effect of the specific locations and to enhance the performance on the imbalanced dataset, respectively. To the best of our knowledge, this is the first model that applies deep learning techniques to correct bias in S2S precipitation from the CFSv2 dataset at national level.

Features used in this work are meteorological indices as well as CFSv2's precipitation data. Results demonstrate that the proposed model outperformed all baselines, both the linear-downscaling technique and the Attention U-Net model. As for the linear-downscaling technique, results reveal an improvement in TCC (13.77%) and an improvement in RMSE (8.65%). The Attention U-Net model achieves improvements in TCC (12.06%) and in RMSE (15.56%). Especially our model shows the highest improvement in the southern region of Thailand which is the most difficult area for the forecasting.

It is important to highlight that our work is tailored for a precipitation forecasting in Thailand. Thus, the meteorological indices are limited and chosen only for Thailand. In future research, the improvement of models can potentially enhanced by training on a longer period of data; assuming that the collection of precipitation data spans a longer period of time, hence increasing the effectiveness of the model.

ACKNOWLEDGMENT

The authors would like to thank Hydro-Informatics Institute (HII) for providing the precipitation dataset used in this study.

REFERENCES

[1] A. Mariotti, P. M. Ruti, and M. Rixen, "Progress in subseasonal to seasonal prediction through a joint weather and climate community effort," *NPJ Climate Atmos. Sci.*, vol. 1, no. 1, p. 4, Mar. 2018, doi: 10.1038/s41612-018-0014-z.

[2] S. Saha et al., "The NCEP climate forecast system version 2," *J. Climate*, vol. 27, no. 6, pp. 2185–2208, Mar. 2014. [Online]. Available: https://journals.ametsoc.org/view/journals/clim/27/6/jcli-d-12-00823.1.xml

[3] H. Hersbach et al., "The ERA5 global reanalysis," *Quart. J. Roy. Meteorol. Soc.*, vol. 146, no. 730, pp. 1999–2049, Jul. 2020. [Online]. Available: https://rmets.onlinelibrary.wiley.com/doi/abs/10.1002/qj.3803

[4] R. Kotamarthi, K. Hayhoe, L. O. Mearns, D. Wuebbles, J. Jacobs, and J. Jurado, *Empirical-Statistical Downscaling*. Cambridge, U.K.: Cambridge Univ. Press, 2021, pp. 82–101.

[5] M. Li, H. Jin, and Q. Shao, "Improvements in subseasonal forecasts of rainfall extremes by statistical postprocessing methods," *Weather Climate Extremes*, vol. 34, Dec. 2021, Art. no. 100384. [Online]. Available: https://www.sciencedirect.com/science/article/pii/S2212094721000748

[6] F. Wang, D. Tian, and M. Carroll, "Customized deep learning for precipitation bias correction and downscaling," *Geosci. Model Develop.*, vol. 16, no. 2, pp. 535–556, Jan. 2023. [Online]. Available: https://gmd.copernicus.org/preprints/gmd-2022-213/

[7] L. Espeholt, S. Agrawal, C. Sønderby, M. Kumar, J. Heek, C. Bromberg, C. Gazen, R. Carver, M. Andrychowicz, J. Hickey, A. Bell, and N. Kalchbrenner, "Deep learning for twelve hour precipitation forecasts," *Nature Commun.*, vol. 13, no. 1, p. 5145, Sep. 2022, doi: 10.1038/s41467-022-32483-x.

[8] Y. Hu, F. Yin, and W. Zhang, "Deep learning-based precipitation bias correction approach for Yin–He global spectral model," *Meteorol. Appl.*, vol. 28, no. 5, p. e2032, Sep. 2021. [Online]. Available: https://rmets.onlinelibrary.wiley.com/doi/abs/10.1002/met.2032

[9] Y. Ji, X. Zhi, L. Ji, Y. Zhang, C. Hao, and T. Peng, "Deep-learning-based post-processing for probabilistic precipitation forecasting," *Frontiers Earth Sci.*, vol. 10, Sep. 2022, Art. no. 978041. [Online]. Available: https://www.frontiersin.org/articles/10.3389/feart.2022.978041

[10] C. Wang, Z. Jia, Z. Yin, F. Liu, G. Lu, and J. Zheng, "Improving the accuracy of subseasonal forecasting of China precipitation with a machine learning approach," *Frontiers Earth Sci.*, vol. 9, May 2021, Art. no. 659310. [Online]. Available: https://www.frontiersin.org/articles/10.3389/feart.2021.659310

[11] J. Hwang, P. Orenstein, J. Cohen, K. Pfeiffer, and L. Mackey, "Improving subseasonal forecasting in the Western U.S. with machine learning," in *Proc. 25th ACM SIGKDD Int. Conf. Knowl. Discovery Data Mining*. New York, NY, USA: Association for Computing Machinery, Jul. 2019, pp. 2325–2335, doi: 10.1145/3292500.3330674.

[12] N. Vigaud, A. W. Robertson, and M. K. Tippett, "Multimodel ensembling of subseasonal precipitation forecasts over North America," *Monthly Weather Rev.*, vol. 145, no. 10, pp. 3913–3928, Oct. 2017. [Online]. Available: https://journals.ametsoc.org/view/journals/mwre/145/10/mwr-d-17-0092.1.xml

[13] D. Specq and L. Batté, "Improving subseasonal precipitation forecasts through a statistical–dynamical approach : Application to the southwest tropical Pacific," *Climate Dyn.*, vol. 55, nos. 7–8, pp. 1913–1927, Oct. 2020, doi: 10.1007/s00382-020-05355-7.

[14] N. Vigaud, M. K. Tippett, J. Yuan, A. W. Robertson, and N. Acharya, "Spatial correction of multimodel ensemble subseasonal precipitation forecasts over North America using local Laplacian eigenfunctions," *Monthly Weather Rev.*, vol. 148, no. 2, pp. 523–539, Feb. 2020. [Online]. Available: https://journals.ametsoc.org/view/journals/mwre/148/2/mwr-d-19-0134.1.xml

[15] A. H. Azman, N. N. A. Tukimat, and M. A. Malek, "Analysis of linear scaling method in downscaling precipitation and temperature," *Water Resour. Manage.*, vol. 36, no. 1, pp. 171–179, Jan. 2022, doi: 10.1007/s11269-021-03020-0.

[16] M. N. Legasa, R. Manzanas, A. Calviño, and J. M. Gutiérrez, "A posteriori random forests for stochastic downscaling of precipitation by predicting probability distributions," *Water Resour. Res.*, vol. 58, no. 4, Apr. 2022, Art. no. e2021WR030272.

[17] D. Long, L. Bai, L. Yan, C. Zhang, W. Yang, H. Lei, J. Quan, X. Meng, and C. Shi, "Generation of spatially complete and daily continuous surface soil moisture of high spatial resolution," *Remote Sens. Environ.*, vol. 233, Nov. 2019, Art. no. 111364. [Online]. Available: https://www.sciencedirect.com/science/article/pii/S0034425719303839

[18] Y. Mei, V. Maggioni, P. Houser, Y. Xue, and T. Rouf, "A nonparametric statistical technique for spatial downscaling of precipitation over high mountain Asia," *Water Resour. Res.*, vol. 56, no. 11, Nov. 2020, Art. no. e2020WR027472. [Online]. Available: https://agupubs.onlinelibrary.wiley.com/doi/abs/10.1029/2020WR027472

[19] H. Xu, C.-Y. Xu, S. Chen, and H. Chen, "Similarity and difference of global reanalysis datasets (WFD and APHRODITE) in driving lumped and distributed hydrological models in a humid region of China," *J. Hydrol.*, vol. 542, pp. 343–356, Nov. 2016. [Online]. Available: https://www.sciencedirect.com/science/article/pii/S0022169416305613

[20] S. H. Pour, S. Shahid, and E.-S. Chung, "A hybrid model for statistical downscaling of daily rainfall," *Proc. Eng.*, vol. 154, pp. 1424–1430, Jan. 2016. [Online]. Available: https://www.sciencedirect.com/science/article/pii/S1877705816319038

[21] S. Tripathi, V. V. Srinivas, and R. S. Nanjundiah, "Downscaling of precipitation for climate change scenarios: A support vector machine approach," *J. Hydrol.*, vol. 330, nos. nos. 3–4, pp. 621–640, Nov. 2006. [Online]. Available: https://www.sciencedirect.com/science/article/pii/S0022169406002368

[22] J. T. Schoof and S. C. Pryor, "Downscaling temperature and precipitation: A comparison of regression-based methods and artificial neural networks," *Int. J. Climatol.*, vol. 21, no. 7, pp. 773–790, Jun. 2001. [Online]. Available: https://rmets.onlinelibrary.wiley.com/doi/abs/10.1002/joc.655

[23] T. Vandal, E. Kodra, and A. R. Ganguly, "Intercomparison of machine learning methods for statistical downscaling: The case of daily and extreme precipitation," *Theor. Appl. Climatol.*, vol. 137, nos. nos. 1–2, pp. 557–570, Jul. 2019. [Online]. Available: https://ui.adsabs.harvard.edu/abs/2019ThApC.137.557V

[24] O. Ronneberger, P. Fischer, and T. Brox, "U-Net: Convolutional networks for biomedical image segmentation," 2015, *arXiv:1505.04597*.

[25] T.-Y. Lin, P. Goyal, R. Girshick, K. He, and P. Dollár, "Focal loss for dense object detection," *IEEE Trans. Pattern Anal. Mach. Intell.*, vol. 42, no. 2, pp. 318–327, Feb. 2020.

[26] P. P. Sreekala, S. V. B. Rao, K. Rajeevan, and M. S. Arunachalam, "Combined effect of MJO, ENSO and IOD on the intraseasonal variability of northeast monsoon rainfall over south peninsular India," *Climate Dyn.*, vol. 51, nos. 9–10, pp. 3865–3882, Nov. 2018, doi: 10.1007/s00382-018-4117-3.

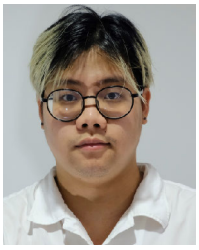

TANATORN FAIJAROENMONGKOL received the B.Sc. degree in electrical engineering from the Department of Electrical Engineering, Faculty of Engineering, Chulalongkorn University, Thailand, in 2019. He is currently pursuing the M.Sc. degree in computer engineering with the Department of Computer Engineering, Faculty of Engineering, Chulalongkorn University. His main research interests include machine learning, deep learning, and image detection.

KANOKSRI SARINNAPAKORN received the B.S. and M.S. degrees in statistics from Kasetsart University, Thailand, the M.S. degree in computer science from Fairleigh Dickinson University, Teaneck, NJ, USA, and the Ph.D. degree in electrical and computer engineering from the University of Miami, Coral Gables, FL, USA. She is an expert in data science, machine learning, and advanced statistical data analysis. She plays a pivotal role as a Researcher and the acting Head of the Climate and Weather Section and the Hydro Data Science Section, Hydro-Informatics Institute (Public Organization). Her primary focus involves developing rainfall prediction models to support the operations of the National Hydro Informatics Data Center, Thailand.

PEERAPON VATEEKUL (Member, IEEE) received the Ph.D. degree from the Department of Electrical and Computer Engineering, University of Miami (UM), Coral Gables, FL, USA, in 2012. He is currently an Associate Professor with the Department of Computer Engineering, Faculty of Engineering, Chulalongkorn University, Thailand. His research interests include machine learning, data mining, deep learning, text mining, big data analytics, natural language processing, and applied deep learning techniques in various domains, such as healthcare, geoinformatics, hydrometeorology, and energy trading.